Sensor networks

Measurement Device of Nondestructive Testing (NDT) of Metanil Yellow Dye Waste Concentration Using Artificial Neural Network Based on Microcontroller

Adhe Lingga Dewi[1], Jatmiko Endro Suseno[2], and Qidir Maulana Binu Soesanto[2]

[1]Master of Physics Study Program, Department of Physics, Faculty of Science and Mathematics, Diponegoro University, Kota Semarang 50275, Indonesia

[2]Department of Physics, Faculty of Science and Mathematics, Diponegoro University, Kota Semarang 50275, Indonesia

Manuscript received 14 June 2022; accepted 14 July 2022. Date of publication 21 July 2022; date of current version 9 August 2022.

Abstract—This research applied the nondestructive testing (NDT) method of the emission gas produced by metanil yellow waste, carbon dioxide (CO_2), and hydrogen (H_2) gases with TiO_2 as a catalyst material to detect the concentration of metanil yellow waste using artificial neural network based on a microcontroller. This device consists of Arduino UNO, LCD 16×2 I2C, MQ-8 H_2 gas sensor, MQ-135 CO_2 gas sensor, BH1750 light sensor, and DHT11 temperature sensor. The concentration of waste is 5–30 mg/L with variations range of 5 mg/L. Meanwhile, the neural network architecture was created using the MATLAB R2018a application. The architecture that owned 25 neurons was chosen due to its performance value with an error of 3.98×10^{-25} and epoch 165. The result of artificial neural network (ANN) training on MATLAB of 4-25-1 architecture contains an error value of 0.024%. The weight and bias values in the training process are programming ANN to Arduino. The testing has an error value of 6.028% and a root-mean-square error of 0.552. Based on the error values, it shows that the training is reaching close to the actual value, it can be concluded that the device can work properly and is practical to use because it does not take long to observe.

Index Terms—Sensor networks, artificial neural networks (ANNs), carbon dioxide (CO_2), hydrogen (H_2), metanil yellow (MY) waste, nondestructive testing (NDT).

I. INTRODUCTION

Azo dye waste caused by industrial activity is one of the factors damaging environmental pollution, especially water. Contamination of water sources due to these dyes causes an unaesthetic view. The presence of these dyes also has a negative impact on the ecosystem in the water and reduces the transmission of sunlight in the water [1], thereby reducing the photosynthetic activity.

One of the azo dyes that are mostly used in the industry is metanil yellow (MY). These dyes are highly implemented in the textile industry [2], soap dyes [3], paper [4], and silk dyeing [5], but it still abused for food and beverage dye coloring. Consuming food contaminated with MY leads to central nervous system disorders [1], cancer in living tissue [6], oxidative stress in various vital organs (such as heart, liver, and kidneys) [7], [8], and lymphocytic leukemia [9]. Therefore, it is important to determine the level of MY in food labels using a detector.

Many researchers conducted research to identify the type and concentration of MY dye waste. In 2019, Das et al. [10] investigates MY in turmeric powder using an electrical impedance spectroscopy technique, the observation is supported by ultraviolet–visible (UV–Vis) absorption spectroscopy and Fourier transform mid-infrared spectroscopy. Kar et al. in 2018 [11] reported the approach to find the adulteration of turmeric with MY by near-infrared spectroscopy coupled with chemometrics. Kourani et al. in 2020 [12] using a multiplate UV–Vis spectrophotometer and attenuated total reflectance–Fourier transform infrared spectroscopy to detect MY. However, the operational complexity and the destructive nature of the sample restrict this analytical method to laboratory purposes and are impractical because it takes a long time to observe.

The method of nondestructive testing (NDT) is relatively easy to determine the concentration of a substance. The advantages of using the NDT method are cost-effective sample testing [13], identification and characterization of defects without changing the material [14], component evaluation without destroying the object tested [15], and running at a short time [16]. To improve system reliability and operation in the NDT method, an artificial neural network (ANN) has been used in several works such as research works about the evaluation of crack depths and angles for pulsed eddy current [17], compressive strength prediction [18], predicting concrete compressive strength [19], removal from aqueous solution by emulsion liquid membrane using ANN [20], and liquid level transmitter using a force resistive sensor [21]. Currently, ANN is widely used in the numerical paradigm due to its adaptive nature, fault tolerance, input progress to output mapping [22], and high-speed processing [23].

The chemical reaction of MY dye waste due to exposure to sunlight is $C_{12}H_{12}O_{11} + HO\bullet \rightarrow CO_2 + H_2$. The gas produced is carbon dioxide gas (CO_2) and hydrogen gas (H_2) [24]. This research applies the NDT method of the emission gas produced by MY dye waste, gases of CO_2 and H_2 with TiO_2 as a catalyst material while employing the intensity of sunlight and ambient temperature to know the environmental conditions. TiO_2 photocatalysts are most often studied because of their ability to break down organic pollutants and even achieve complete mineralization [25]. The correlation between input and output is captured using the ANN method.

II. RESEARCH METHOD

A. Preparation of Waste Sample Solution

Preparation of the MY solution was carried out by homogenizing 0.1 g of MY powder into 100 mL of distilled water to obtain 1000 mg/L MY mother liquor. This mother liquor was then diluted into six variations of 5, 10, 15, 20, 25, and 30 mg/L.

Corresponding author: Jatmiko Endro Suseno (e-mail: jatmikoendro@lecturer.undip.ac.id)

Associate Editor: I. Papautsky.

Digital Object Identifier 10.1109/LSENS.2022.3192865

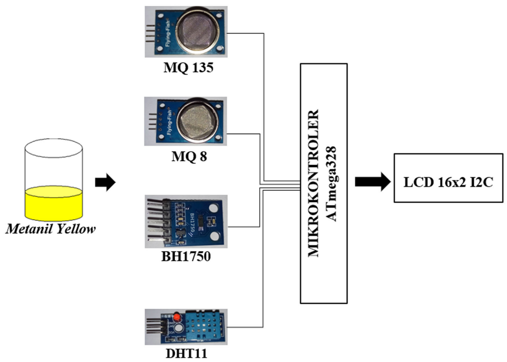

Fig. 1. Device diagram.

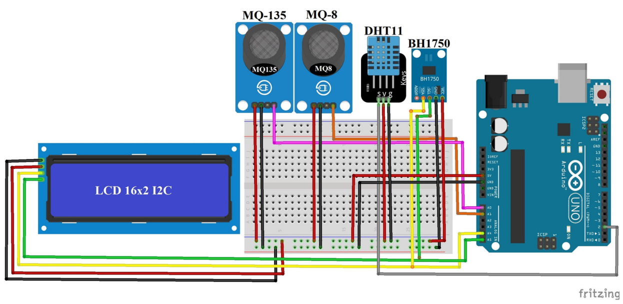

Fig. 2. Electronics circuit system.

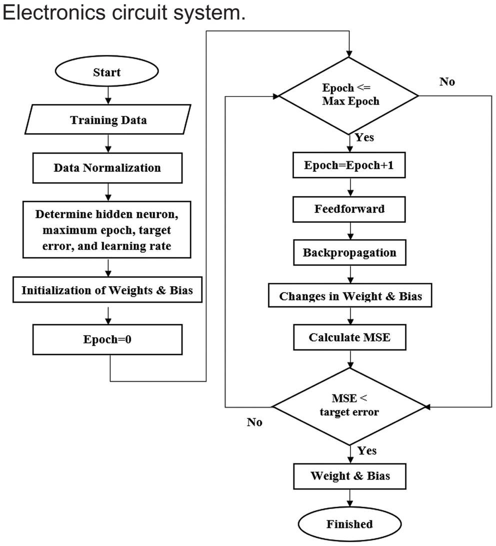

Fig. 3. ANN training flowchart in MATLAB.

B. Sensor Data Acquisition

This device is composed of Arduino UNO, LCD 16×2 I2C, MQ-8 H2 gas sensor, MQ-135 CO2 gas sensor, BH1750 light sensor, and DHT11 temperature sensor, as shown in Fig. 1. Arduino UNO works as a sensor data control center whose programming uses the Arduino IDE. The MQ-8 H2 gas sensor detects hydrogen gas, and the MQ-135 CO2 gas sensor detects carbon dioxide while the BH1750 light sensor measures the light intensity and the DHT11 temperature sensor measures temperature. The measurement result will be displayed on an LCD 16×2 I2C that looks like H_2 rate (ppm), CO_2 rate (ppm), light intensity (lux), and temperature (°C). The electronic circuit of the system is made using a fritzing application, as shown in Fig. 2.

C. Neural Network Training on MATLAB

The flowchart of the MATLAB ANN training process is shown in Fig. 3.

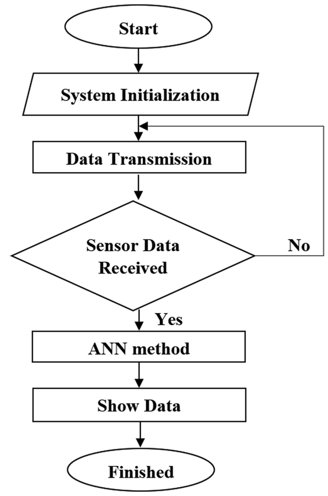

Fig. 4. ANN testing flowchart on Arduino.

Neural network training on MATLAB is starting by varying the hidden layer values from 5, 10, 15, 20, 25, and 30. The first stage before starting the training process is the normalization of the data, adjusting the number of neurons, and the methods used for the network architecture. In this process, the data will be arranged to produce errors and epochs that match the maximum target value of error and epoch values. If the error and epoch values have not reached the smallest value yet, the process will be repeated from the training network stage. Afterward, if the error and epoch values have fulfilled the target, the weight and bias values will be stored for the next Arduino program.

D. Neural Network Testing on Arduino

The flow diagram of the ANN testing process on Arduino is shown in Fig. 4.

This stage is carried out to determine the error value of the target with the actual target and to ascertain the feasibility of the device. The sensor transmits data then processed by the ANN method. The output data will appear on an LCD 16×2 I2C that comprises parameters of H_2 rate (ppm), CO_2 (ppm), light intensity (lux), and temperature (°C).

The functions for calculating the ANN test are as follows:

1) Input normalization:
ANN training data in MATLAB must be normalized first with an interval of 0.1–0.9 with

$$X' = 0.8\left(\frac{X-a}{b-a}\right) + 0.1\,. \tag{1}$$

2) The sum of the bias values of the neurons and the results of multiplying inputs with the associated weights

$$\text{Neuron1} = \left(\sum_{i=1}^{n} Ii \times wi\right) + B_1 \tag{2a}$$

$$\text{Neuron2} = \left(\sum_{i=1}^{n} Ii \times wi\right) + B_2 \tag{2b}$$

and so on.

3) Hidden layer activation:

$$\text{activation} = \text{activation}\ (\text{Neuron1}, \ldots, \text{Neuron } n)\,. \tag{3}$$

4) Multiply the hidden layer activation results with each associated output layer weight and sum with output bias

$$\text{Output} = \left(\sum_{i=1}^{n} \text{Neuron } i \times wi\ \text{output}\right) + B\ \text{output}. \tag{4}$$

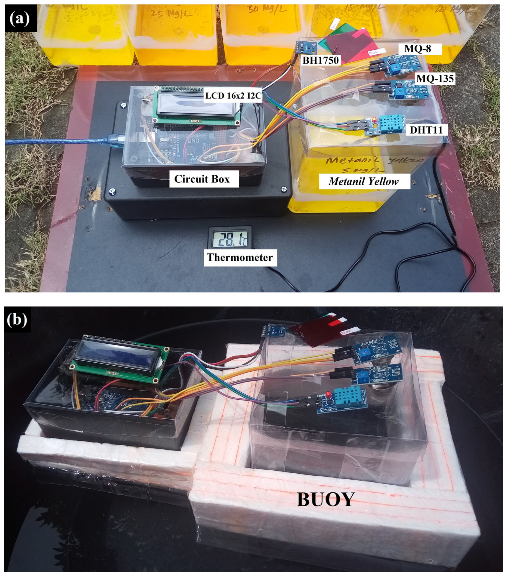

Fig. 5. View of the device. (a) Top view. (b) Realization device.

5) Output denormalization:

$$X = \left(\frac{(X' - 0.1)\,(b - a)}{0.8} \right) + a \tag{5}$$

where X' = Normalized data, X = Parameter data, a = Minimum data, b = Maximum data, I = Input data, w = weight, and B = bias.

E. Realization Device

The front view of the device has four sensors placed on the cover mica and LCD 16×2 I2C to read the measurement results. The cover mica functions as a cover for the MY solution container to which the catalyst material (TiO_2) has been added. The MQ-8 H2 gas sensor and MQ-135 CO2 gas sensor are posited face down or oriented to the MY solution box while the BH1750 light sensor and DHT11 temperature sensor are facing toward the top of the cover mica, as shown in Fig. 5.

III. RESULT AND DISCUSSION

This research was conducted to obtain an NDT measuring device for the concentration of MY dye waste based on the chemical reaction output parameters using an ANN microcontroller based. Sensor data retrieval was performed at each concentration of MY solution 18 times with time duration of 10 min (600 s). The data are the values of H_2 (ppm), CO_2 (ppm), light intensity (lux), and temperature (°C) and then used as input data for training ANNs in MATLAB. The ANN architecture was made using the MATLAB R2018a application with the *nntool* command. The architecture is constructed by varying the hidden layer values to get the error values and the smallest epoch that will be considered in the next process. The network type is back-propagation with a training function, such as Levenberg–Marquardt training (Trainlm), adaptation learning function, i.e., LearnGDM, performance function, i.e., the mean-squared error, a transfer function of tansig in the output layer, applying maximum iteration of 10 000, and the goal (tolerance error) is 0.

Table 1 shows the comparison of error and epoch values for each architecture. Based on the table, the architecture with 25 neurons has a better performance value with the smallest error value of 3.98E-25 with 165 epochs. The ANN architecture is shown in Fig. 6 .

The results of training on architecture 4-25-1 attained performance graphs and regression values. It can be observed at the green circle point in Fig. 7 that the best validation performance on the graph is 7.048 in the fifth epoch.

TABLE 1. Network Architecture Comparison

No	Architecture	*Error*	*Epoch*	Hidden layers
1.	4-5-1	0,509	1009	5
2.	4-10-1	0,141	1000	10
3.	4-15-1	$2{,}36 \times 10^{-24}$	359	15
4.	4-20-1	$2{,}39 \times 10^{-19}$	139	20
5.	4-25-1	$3{,}98 \times 10^{-25}$	165	25
6.	4-30-1	$1{,}47 \times 10^{-23}$	164	30

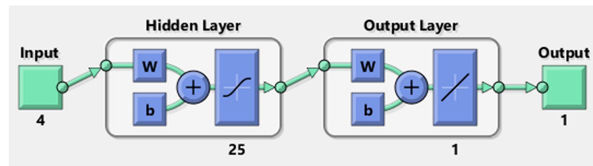

Fig. 6. Network architecture of 4-25-1.

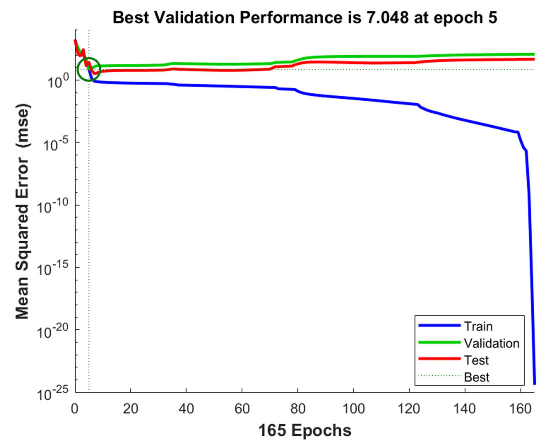

Fig. 7. Architecture performance of 4-25-1.

The results of the MATLAB ANN training on the 4-25-1 architecture produce a regression value, which is shown in Fig. 8. The regression value at the training data is $R = 0.96552$, the regression value at the test is $R = 0.96134$, the regression value at the validation is $R = 0.96277$, and the overall regression value is $R = 0.95086$.

The regression results indicate that the training data have good accuracy and linearity because the training output value is approximately close to the actual target value. The concentration value of the training MY dye waste was compared with the target or actual MY dye waste concentration value and the average error value was 0.024%. Based on training in MATLAB, the weight and bias values involved 100 hidden layer weight values, 25 output layer weight values, 25 hidden layer bias values, and 1 output layer bias value. Thereafter, the weight and bias values are processed for programming ANN on the Arduino platform.

The calculation of the ANN testing on Arduino is done using the weights and bias values that have been generated from the ANN training in MATLAB and using (1)–(5). Data were collected 10 times for each concentration of 3, 8, 17, 26, and 35 mg/L with a time duration of 10 min (600 s). ANN testing on Arduino is committed by entering the input value in the existing program; then, the value that has been detected will be processed in the program until the solution concentration value is taken. The test results are shown in Fig. 9.

Based on the comparison graph of the actual waste concentration with the test device in Fig. 9, it can be observed that the concentration value of the measurement results approaches the actual concentration value. Although there are some points that indicate a quite significant deviation such as at concentrations of 7, 26, and 35 mg/L at 6000 s, respectively, there was a difference of 0.8 mg/L. The concentration value of the MY dye waste from the Arduino was further compared with the actual MY dye waste concentration value and the average relative error value was 6.028%. For comparison, use

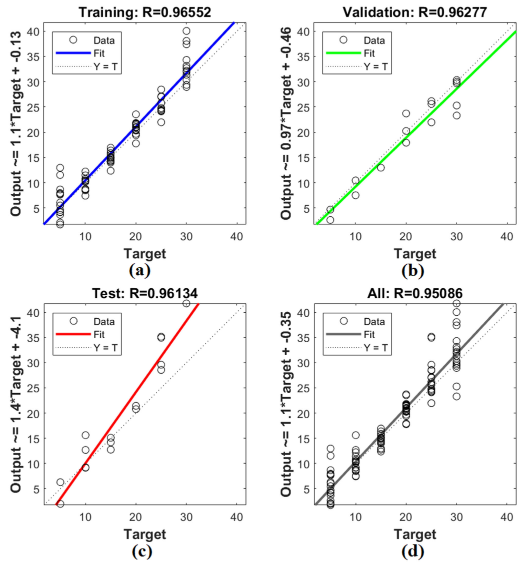

Fig. 8. Architecture regression of 4-25-1. (a) Training. (b) Validation. (c) Test. (d) All.

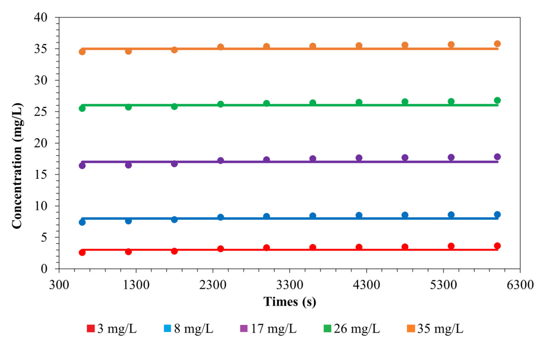

Fig. 9. Comparison graph of actual waste concentration with the test device, where lines are actual value and dots are measurement results.

the calculation of a root-mean-square error (RMSE) with the result of 0.552, the RMSE value is good because the value is very small (close to 0). This RMSE value is smaller than that in the research by Das et al. [10], which has an RMSE value of 0.96–0.99. Thus, this result shows that the error value from the ANN test is near the actual value. In this case, there are two things that affect the magnitude of the error value: 1) the minimum input data quantity and 2) environmental conditions that may cause the light intensity and temperature fluctuating values.

IV. CONCLUSION

The measurement device of NDT of MY dye waste concentration using the ANN based on the microcontroller has been composed. The results of the ANN training on MATLAB using the 4-25-1 architecture derived an error value of 0.024% while testing on Arduino obtained an error value of 6.028% and RMSE 0.552. Based on the error values in the training and testing process, it states that the training process is nearby reached the actual target value and it can be concluded that the device can function properly. The use of the NDT method in this study helps us to not directly sampling of the original waste, which needs a long process, precisely cheaper, and real-time testing.

ACKNOWLEDGMENT

The authors would like to thank Instrumentation and Computing Laboratory, Department of Physics, Diponegoro University, for their valuable contribution to this measurement.

REFERENCES

[1] A. Malviya, D. K. Jaspal, and S. Khamparia, "Kinetics studies on the adsorption of methyl orange and metanil yellow onto bottom ash: A comparative account," *Water Sci. Technol.*, vol. 80, pp. 1844–1850, 2019.

[2] M. Nurdin et al., "Photocurrent responses of metanil yellow and Remazol Red B organic dyes by using TiO_2/Ti electrode," in *Proc. IOP Conf. Ser.: Mater. Sci. Eng.*, 2018, Art. no. 012048.

[3] F. N. A. Muliadi et al., "Biostimulation of microbial communities from Malaysian agricultural soil for detoxification of metanil yellow dye; a response surface methodological approach," *Sustainability*, vol. 13, 2020, Art. no. 138.

[4] K. C. Lai et al., "Ice-templated graphene oxide/chitosan aerogel as an effective adsorbent for sequestration of metanil yellow dye," *Bioresource Technol.*, vol. 274, pp. 134–144, 2019.

[5] B. O. Isiuku and B. I. Nwabueze, "Aqueous phase adsorption of metanil yellow on phosphoric acid-activated carbon prepared from GMELINA ARBOREA bark," *J. Chem. Soc. Nigeria*, vol. 44, pp. 030–040, 2019.

[6] A. Singh and A. M. Siddiqui, "Andgerous food items," *Significances Bioeng. Biosci.*, vol. 2, no. 1, p. 4, 2018.

[7] W. M. Elwan, "Effect of long-term administration of metanil yellow on the structure of cerebellar cortex of adult male albino rat and the possible protective role of anise oil: A histological and immunohistochemical study," *Egyptian J. Histol.*, vol. 41, pp. 27–38, 2018.

[8] R. N. Dome, S. A. Hazra, D. E. Ghosh, and S. U. Ghosh, "Beneficial effects of ethanolic leaf extract of Coriandrum sativum on metanil yellow induced alteration in activity of catalase and level of lipid peroxidation in hercine cardiac tissue," *Int. J. Pharm. Pharmaceut. Sci.*, vol. 9, pp. 203–209, 2017.

[9] S. Dhakal, K. Chao, J. Qin, M. Kim, W. Schmidt, and D. Chan, "Detection of metanil yellow contamination in turmeric using FT-Raman and FT-IR spectroscopy," in *Proc. Sens. Agriculture Food Qual. Saf. VIII*, 2016, pp. 28–36.

[10] C. Das et al., "Impedimetric approach for estimating the presence of metanil yellow in turmeric powder from tunable capacitance measurement," *Food Anal. Methods*, vol. 12, pp. 1017–1027, 2019.

[11] S. Kar, B. Tudu, A. K. Bag, and R. Bandyopadhyay, "Application of near-infrared spectroscopy for the detection of metanil yellow in turmeric powder," *Food Anal. Methods*, vol. 11, pp. 1291–1302, 2018.

[12] K. Kourani, N. Kapoor, A. Badiye, and R. K. Shukla, "Detection of synthetic food color 'Metanil yellow' in sweets: A systematic approach," *JPC—J. Planar Chromatography—Modern TLC*, vol. 33, pp. 413–418, 2020.

[13] A. Sophian, G. Tian, and M. Fan, "Pulsed eddy current non-destructive testing and evaluation: A review," *Chin. J. Mech. Eng.*, vol. 30, pp. 500–514, 2017.

[14] S. K. Dwivedi, M. Vishwakarma, and A. Soni, "Advances and researches on non destructive testing: A review," *Mater. Today: Proc.*, vol. 5, pp. 3690–3698, 2018.

[15] S. Gholizadeh, "A review of non-destructive testing methods of composite materials," *Procedia Struct. Integrity*, vol. 1, pp. 50–57, 2016.

[16] O. Tsioulou, A. Lampropoulos, and S. Paschalis, "Combined non-destructive testing (NDT) method for the evaluation of the mechanical characteristics of ultra high performance fibre reinforced concrete (UHPFRC)," *Construction Building Mater.*, vol. 131, pp. 66–77, 2017.

[17] F. Nafiah, A. Sophian, M. R. Khan, and I. M. Z. Abidin, "Quantitative evaluation of crack depths and angles for pulsed eddy current non-destructive testing," *NDT E Int.*, vol. 102, pp. 180–188, 2019.

[18] A. Poorarbabi, M. Ghasemi, and M. Azhdary Moghaddam, "Concrete compressive strength prediction using neural networks based on non-destructive tests and a self-calibrated response surface methodology," *J. Nondestruct. Eval.*, vol. 39, pp. 1–11, 2020.

[19] M. Bonagura and L. Nobile, "Artificial neural network (ANN) approach for predicting concrete compressive strength by SonReb," *Struct. Durability Health Monit.*, vol. 15, pp. 125, 2021.

[20] A. Fetimi et al., "Optimization and prediction of safranin-O cationic dye removal from aqueous solution by emulsion liquid membrane (ELM) using artificial neural network-particle swarm optimization (ANN-PSO) hybrid model and response surface methodology (RSM)," *J. Environ. Chem. Eng.*, vol. 9, 2021, Art. no. 105837.

[21] A. Lata and N. Mandal, "ANN-based liquid level transmitter using force resistive sensor for minimisation of hysteresis and non-linearity error," *IET Sci., Meas., Technol.*, vol. 14, pp. 923–930, 2020.

[22] D. Wang, H. He, and D. Liu, "Intelligent optimal control with critic learning for a nonlinear overhead crane system," *IEEE Trans. Ind. Inform.*, vol. 14, no. 7, pp. 2932–2940, Jul. 2017.

[23] N. Izeboudjen, C. Larbes, and A. Farah, "A new classification approach for neural networks hardware: From standards chips to embedded systems on chip," *Artif. Intell. Rev.*, vol. 41, pp. 491–534, 2014.

[24] B. G. Bhernama, S. Safni, and S. Syukri, "Degradasi zat warna metanil yellow dengan penyinaran matahari and penambahan katalis TiO_2-SnO_2," *Lantanida J.*, vol. 3, pp. 116–126, 2017.

[25] M. Umar and H. A. Aziz, "Photocatalytic degradation of organic pollutants in water," *Org. Pollutants—Monit., Risk, Treat.*, vol. 8, pp. 196–197, 2013.